ANL/RE/CP-101101

High Fidelity Thermal-Hydraulic Analysis Using CFD and Massively Parallel Computers

Contact Person:

David P. Weber*
Associate Division Director
Reactor Engineering Division
9700 S. Cass Ave., RE/208
Argonne, IL 60439
(630) 252-8175
(630) 252-4780 FAX
dpweber@anl.gov

*This work was performed under the auspices of the U.S. Department of Energy, Office of Technology Support Programs, under Contract No. W-31-109-ENG-38.

re060dwcover.doc

DISCLAIMER

High Fidelity Thermal-Hydraulic Analysis Using CFD and Massively Parallel Computers

D. P. Weber and T.Y.C. Wei
Reactor Engineering Division
Argonne National Laboratory
Argonne, IL
dpweber@anl.gov; tycwei@anl.gov

R. A. Brewster
adapco
Melville, NY
rbrew@adapco.com

Daniel T. Rock and Rizwan-uddin
Department of Nuclear Engineering
University of Illinois
Urbana, IL
drock@students.uiuc.edu; rizwan@uiuc.edu

Abstract

Thermal-hydraulic analyses play an important role in design and reload analysis of nuclear power plants. These analyses have historically relied on early generation computational fluid dynamics capabilities, originally developed in the 1960s and 1970s. Over the last twenty years, however, dramatic improvements in both computational fluid dynamics codes in the commercial sector and in computing power have taken place. These developments offer the possibility of performing large scale, high fidelity, core thermal hydraulics analysis. Such analyses will allow a determination of the conservatism employed in traditional design approaches and possibly justify the operation of nuclear power systems at higher powers without compromising safety margins. The objective of this work is to demonstrate such a large scale analysis approach using a state of the art CFD code, STAR-CD, and the computing power of massively parallel computers, provided by IBM.

A high fidelity representation of a current generation PWR was analyzed with the STAR-CD CFD code and the results were compared to traditional analyses based on the VIPRE code. Current design methodology typically involves a simplified representation of the assemblies, where a single average pin is used in each assembly to determine the hot assembly from a whole core analysis. After determining this assembly, increased refinement is used in the hot assembly, and possibly some of its neighbors, to refine the analysis for purposes of calculating DNBR. This latter calculation is performed with sub-channel codes such as VIPRE. The modeling simplifications that are used involve the approximate treatment of surrounding assemblies and coarse representation of the hot assembly, where the subchannel is the lowest level of discretization.

In the high fidelity analysis performed in this study, both restrictions have been removed. Within the hot assembly, several hundred thousand to several million computational zones have been used, to accurately determine cross-flow and mixing effects within the subassembly. This analysis also provides detailed thermal profiles for more accurate assessment of thermal conditions such as

approach to local boiling. The second restriction was also removed by using similar level high fidelity models in the surrounding subassemblies. Thus, there was no need for using simplified representative pin analyses in the surrounding assemblies and the correct inter-assembly flows were calculated directly.

Based on initial quarter assembly calculations of 500,000 and 4M cells in the hot quarter assembly, it was shown that energy balances were accurate and averaged exit conditions matched VIPRE analyses. The 500K cell calculations were sufficiently accurate that this modeling detail was used for subsequent multiple assembly analyses. This "whole core" calculation was performed for 30+ assemblies with increased spatial discretization in the axial direction to better represent grid spacer effects, resulting in 240 million CFD computational zones. Calculations were performed on a 200 processor IBM SP massively parallel system. Comparison to VIPRE results showed differences in the peak temperatures of approximately 10F. Steady state calculations were performed in approximately 50 hours for the 240M node case on the 200 processor IBM SP.

The high fidelity, 3-D, whole core subchannel analyses described above utilized a porous media representation of the spacer grids and mixing vanes. To determine appropriate flow coefficients for the porous media model, high fidelity CFD models of the spacer grid can also be performed. Starting from a detailed CAD representation of the grid spacer, a CFD model of a single grid has been developed using the automatic meshing tool of STAR-CD, known as SAMM. The resulting model consisted of more than 10M cells. This model was run to convergence using a 16 processor IBM SP system. Results of these detailed spacer grid analyses at different flow rates can then be used to fit appropriate pressure drop correlations in the porous media model.

The results of these calculations demonstrate the ability of large scale, high fidelity CFD calculations to perform core design and reload analysis in a reasonable amount of time on massively parallel computers. This approach provides quantitative detail on the flow implications of proposed spacer grids and mixing vanes and provides necessary porous media flow coefficient information for subsequent whole core calculations. The fine detail multiple assembly calculation demonstrates the ability to perform high fidelity design calculations to more accurately determine thermal conditions and safety margins. Such detailed thermal hydraulic analyses with well established commercial CFD codes offer the possibility of building a fully integrated neutronic-thermal hydraulic design capability.

1 Introduction

Thermal-hydraulic analyses play an important role in design and reload analysis of nuclear power plants. These analyses have historically relied on early generation computational fluid dynamics capabilities, originally developed in the 1960s and 1970s. Over the last twenty years, however, dramatic improvements in both computational fluid dynamics codes in the commercial sector and in computing power have taken place. These developments offer the possibility of performing large scale, high fidelity, core thermal hydraulics analysis. Such analyses will allow a determination of the conservatism employed in traditional design approaches and possibly justify the operation of nuclear power systems at higher powers without compromising safety margins. The objective of this work is to demonstrate such a large scale analysis approach using a state of the art CFD code, STAR-CD, and the computing power of massively parallel computers, provided by IBM.

The nuclear industry has made effective use of advanced modeling and simulation in the design, operation and optimization of nuclear power plants. In the area of thermal-hydraulics, the industry has developed, validated and applied numerous codes to predict the behavior of the system under normal, off-normal and accident conditions. Key industry issues such as cost reduction, power uprates, and evolving designs are providing the motivation for refined analysis, including three-dimensional representation of core and vessel [Agee 1998, Boatwright 1998]. In the future, very large problems will be run routinely because of the evolving modeling fidelity of advanced thermal-hydraulics analysis tools and reduction in computing time due to advancements in computer technology. Nuclear industry thermal-hydraulic codes and general-purpose computational fluid dynamics (CFD) capability combined with parallel computing architectures are expected to play prominent roles in addressing such problems and providing an advanced analysis environment.

In a previous paper [Weber 1999], a preliminary investigation of the power of modern CFD codes and massively parallel computing was reported. In this work, a high fidelity model of 1/8 of a reactor core was modeled to demonstrate the capability of modern software and hardware systems to address important problems in the nuclear industry. The preliminary investigation has been extended to examine thermal hydraulic performance in greater detail and to examine the power of these tools to address very large computational problems of hundreds of millions of computational zones. This higher fidelity model includes a representation of the spacer grids and mixing vanes using a porous media approach. Modern CFD methods, though, have the ability to model in detail the flow patterns within and around such structures. Resolution of the flow details in these structures, however, requires a fine computational structure for prediction of appropriate pressure drops and turbulence effects. This paper will also illustrate some of these effects, which are based on multi-million cell representations of the spacer grids and mixing vanes. The inclusion of this level of detail in whole core calculations is, at the present time, not possible. Nonetheless, the use of CFD to estimate from first principles the hydrodynamic effects of the flow and thermal enhancing devices, which can then be represented in whole core calculations, shows the power of CFD and parallel computing to provide a consistent and integrated picture of thermal hydraulic behavior. This approach of coupling high fidelity component models to high fidelity system level models is becoming more common in many industrial applications [Lang 1997] and it will illustrate how the nuclear industry can also benefit from such an approach.

2 Computational Fluid Dynamics and High Performance Computing

CFD has evolved rapidly over the last 20 years [Ferziger 1997], aided by the evolution of modern high performance computing architectures. Although initial CFD efforts were limited to simpler representations of the flow equations, such as the Euler equations, and geometric dimensionality was often limited to two-dimensions, including axisymetric flows, modern CFD techniques attempt to analyze problems with complex physics in three dimensional space, for steady-state or transient applications. Modern codes begin with the full set of Navier-Stokes equations, including multi-component fluid and multi-phase effects. Various differencing techniques of the fundamental conservation equations are performed, based on finite difference, finite volume, or finite element techniques. Special attention is placed on numerical representations that accurately represent the differential equations, to insure consistency, accuracy and numerical stability in the numerical solution. The resulting set of algebraic equations may be solved by direct or iterative matrix solvers. Most commercial codes rely on the iterative techniques, where techniques such as incomplete LU decomposition, alternating direction (ADI) methods, conjugate gradient methods, multi-grid methods, etc. are employed.

The demonstration calculations illustrated below were performed with STAR-CD, a commercial CFD code [Computational Dynamics 1999]. This code is representative of the state-of-the-art in modern CFD codes. STAR-CD is a 3-D, single and multiphase CFD code based on an unstructured grid. It allows the use of a wide range of cell shapes that make the code amenable to a variety of efficient grid generation strategies for complex geometries. It contains both a Lagrangian and an Eulerian multi-fluid model and allows the computation of both steady and unsteady flows.

Turbulence can be simulated in STAR-CD with a number of models including the k-ε model with wall functions, and the so-called "two-layer" approach which implements a variety of alternate models in the boundary layer cells. The code can account for a variety of body forces including those due to buoyancy and rotation, as well as for the effect of buoyancy on turbulence. Analyses can be run on multiple processors (using domain decomposition methods); and in a number of cases, the code has been run on as many as 256 processors. Many users employ parallel processing in STAR-CD on a routine basis.

Various options are available for the spatial discretization of the convective terms. In this study, the first-order upwind-differencing scheme was used, while the diffusive terms were discretized by a central-difference scheme, which is second order accurate. The iterative solution of the steady conservation equations was accomplished using the SIMPLE algorithm [Patankar 1980] together with STAR-CD's conjugate-gradient solvers. To ensure numerical stability, SIMPLE requires under-relaxation of all field variables, especially pressure.

3 Sub-Channel Analysis

3.1 Sub-Channel Analysis Methodology

Thermal-hydraulic analyses are performed to insure that the reactor core and associated coolant, control and protection systems have appropriate margins to ensure that specified acceptable fuel design limits are not exceeded during any condition of normal operation, including the effects of anticipated operational occurrence. To provide these assurances, thermal-hydraulic sub-channel analysis tools such as THINC-IV [Chelemer 1976], COBRA [Wheeler 1976], VIPRE [NP-2511-CCM 1983] and TORC [TORC-Code 1975] have been developed and are extensively used by utilities and vendors in design and reload analysis [Swindlehurst 1995]. These tools must be considered as a mature analysis technology that has met the needs of reload design. However, in the current economic environment, the demand for additional power without decreasing DNB margin motivates assessment of new technology for fuel assembly design and core reload design to reduce cost and improve quality of fuel performance.

VIPRE (Versatile Internals and Component Program for Reactors; EPRI) is a general-purpose thermal-hydraulic sub-channel analysis tool developed by the Electric Power Research Institute (EPRI). It is most applicable for nuclear reactors in normal operational conditions, operational transients, and events of moderate severity. For given conditions, VIPRE evaluates the minimum departure from nucleate boiling ratio (MDNBR). VIPRE is specifically tailored for use by nuclear utilities and is approved by the Nuclear Regulatory Commission (NRC) for reactor thermal hydraulics.

VIPRE calculations are performed by dividing a domain into quasi-one-dimensional channels (with cross-flow between channels handled in a mechanistic manner), and solving for channel-averaged

values of fluid enthalpy, axial flow rate, momentum pressure drop, and lateral flow per unit length. Flow fields are taken as incompressible and homogeneous though models are available to incorporate sub-cooled boiling and liquid-vapor slip. VIPRE is routinely used by utilities to simulate 1/8th or 1/4th of cylindrical reactor cores. Such simulations are carried out with finer details in the hot fuel bundle than elsewhere in the core, which serves the purpose of the utilities reasonably well.

3.2 High Fidelity Sub-Assembly Analysis with CFD

A high fidelity representation of a current generation PWR was analyzed with the STAR-CD CFD code and the results were compared to traditional analyses based on the VIPRE code. As noted above, design methodology typically involves a simplified representation of the assemblies, where a single average pin is used in each assembly to determine the hot assembly from a whole core analysis. After determining this assembly, increased refinement is used in the hot assembly, and possibly some of its neighbors, to refine the analysis for purposes of calculating DNBR. This latter calculation is performed with sub-channel codes such as VIPRE. The modeling simplifications that are used involve the approximate treatment of surrounding assemblies and coarse representation of the hot assembly, where the subchannel is the lowest level of discretization.

In the high fidelity analysis performed in this study, both traditional restrictions have been removed. Within the hot assembly, several hundred thousand to several million computational zones have been used, to accurately determine cross-flow and mixing effects within the subassembly. This analysis also provides detailed thermal profiles for more accurate assessment of thermal conditions such as approach to local boiling. The second restriction was also removed by using similar level high fidelity models in the surrounding subassemblies. Thus, there was no need for using simplified representative pin analyses in the surrounding assemblies and the correct inter-assembly flows were calculated directly.

To establish the required level of modeling detail, several calculations were made for one quarter of one subassembly. Figure 1 shows the geometry of a quarter subassembly of a large (3800 MWt) U.S. pressurized water reactor (PWR). The PWR fuel vendor subassembly design consists of a 16 x 16 pin bundle with five large control rod guide tubes. The quarter section selected for analysis has 59 fuel pins, one quarter of the central control guide tube and one of the corner control guide tubes, resulting in a total of 79 subchannels, which are labeled in Figure 1 for later reference. The inter-assembly water gap was explicitly modeled but the control rod cooling water flow was neglected.

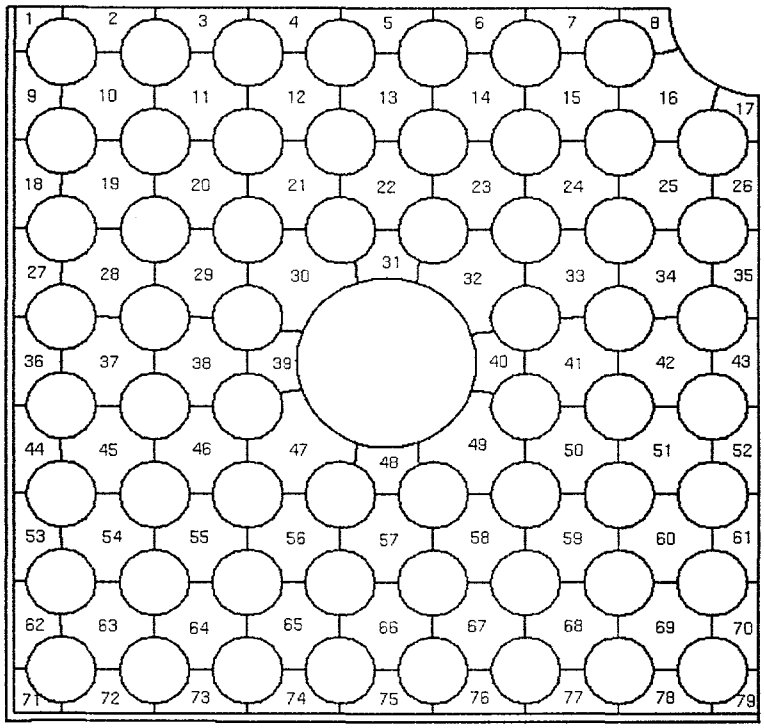

Figure 1. Geometry of ¼ subassembly used in STAR-CD analysis

Power and flow conditions selected for these analyses are typical of a hot assembly during a burnup cycle. However, while pin radial power factors are taken from a typical fuel cycle calculation, the total assembly power has been adjusted so that the mixed mean outlet temperature in the hot channel is 9°F below saturation. A typical chopped cosine with an appropriate axial power peaking factor is used for the axial power distribution. A total subassembly inlet flow condition is imposed.

This is a hot subassembly with high power and low flow. In the preliminary investigation [Weber 1999] the spacer grids were removed as well as the inlet and outlet regions of the fuel subassembly design. The specific heat and density of the coolant were assumed to vary with temperature at the operating pressure (~2250 psia), and all other coolant properties were constant.

Utilizing these input and boundary conditions, several calculations were made. The first calculation was made using the subassembly performance thermal-hydraulic code VIPRE.

The quarter subassembly was modeled in VIPRE with all 79 subchannels. The axial heat flux profile was specified using the VIPRE 'chopped cosine' flux shape option with a peak of 1.47 and an average rod power of approximately 60.5 kW/rod. The inlet velocity was uniform at 14.79 ft/s (4.51 m/s) and an inlet temperature of 555.28F (290.71C) was specified. There were 44 axial nodes in the z-direction of each subchannel. VIPRE then computed the averaged velocity and temperature in each subchannel for each of the axial nodes.

In addition, two calculations were made using the STAR-CD CFD code. The two STAR-CD calculations were made using two different computational mesh densities. Comparison of the results from the two different models will indicate the sensitivity of the results to the mesh density.

The first model is shown in Figure 2 and consists of a total of 473,600 computational cells (200 layers in the axial direction by 2,368 cells per layer). The analysis for this model was run in serial mode on an IBM RS/6000 Model 595 workstation.

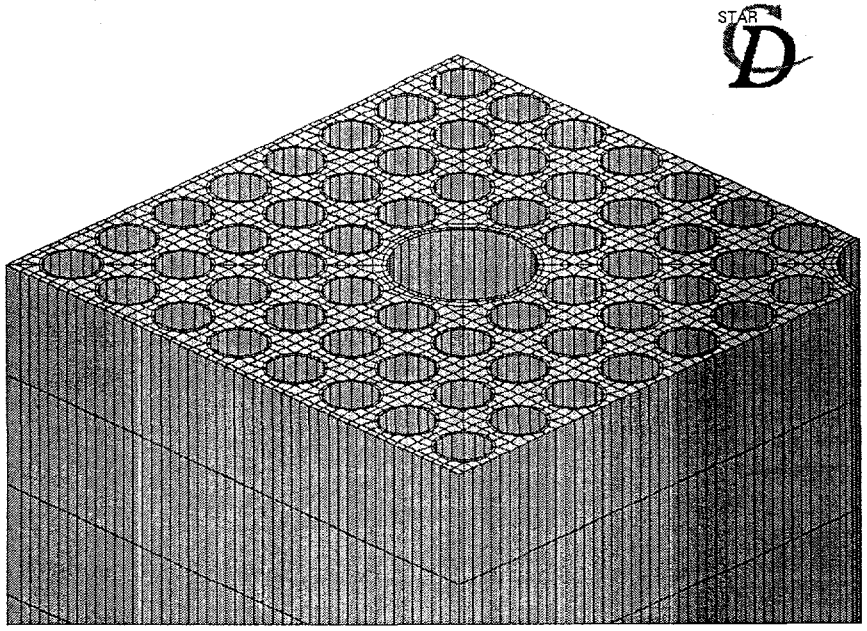

Figure 2. STAR-CD subchannel mesh for 473,600 mesh cells

The second model shown in Figure 3 was a refined version of the first, and consisted of a total of 3,765,600 computational cells (400 layers in the axial direction by 9,414 cells per layer). This model was run in parallel on eight IBM SP nodes.

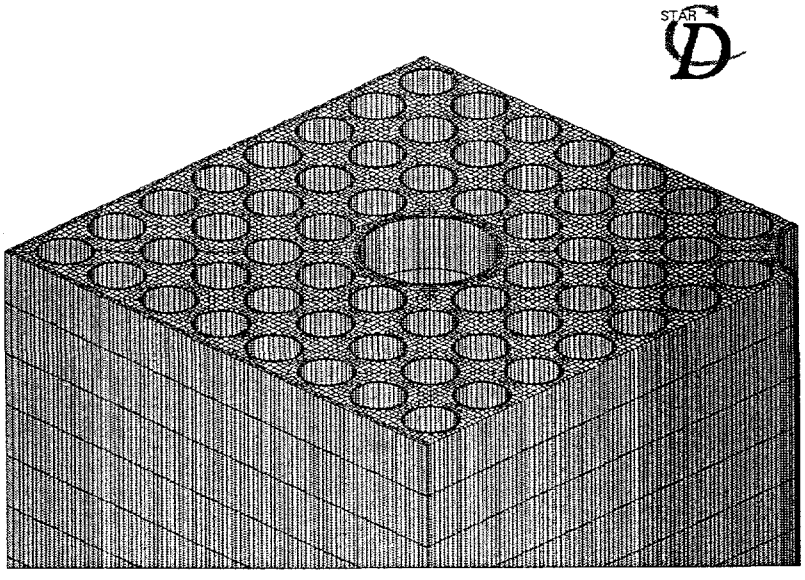

Figure 3. STAR-CD subchannel mesh for ,3765,600 mesh cells

A comparison between the results obtained with STAR-CD and VIPRE is shown in Figures 4 and 5. It can be seen that the two solutions generally agree very well. This was largely expected, since the coolant mass flow rates and power input were the same for the two models. Everything else being equal, the two codes should, on average, predict the same outlet temperatures. Figure 6 shows the temperature contours at the outlet plane from STAR-CD for the quarter subassembly calculation.

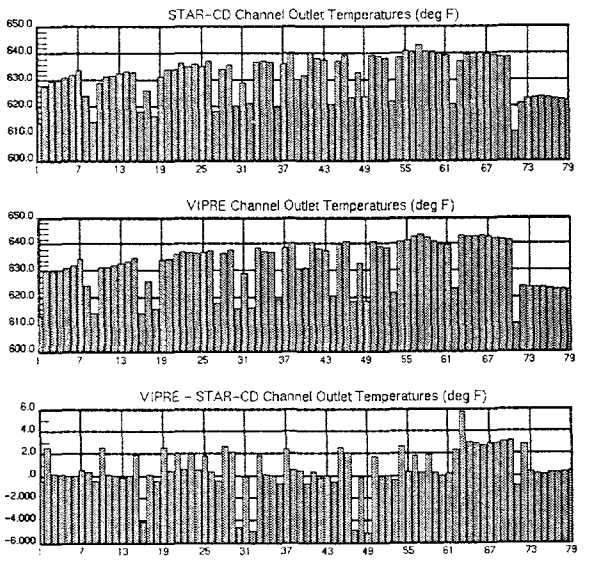

Figure 4. Comparison of average channel outlet temperatures between STAR-CD and VIPRE for small STAR mesh

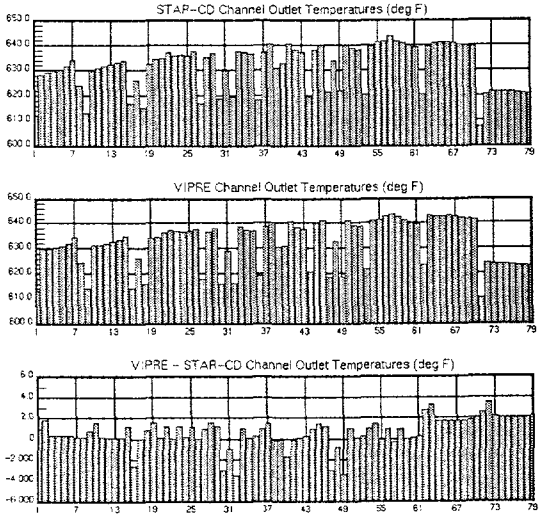

Figure 5. Comparison of average channel outlet temperatures between STAR-CD and VIPRE for large STAR mesh

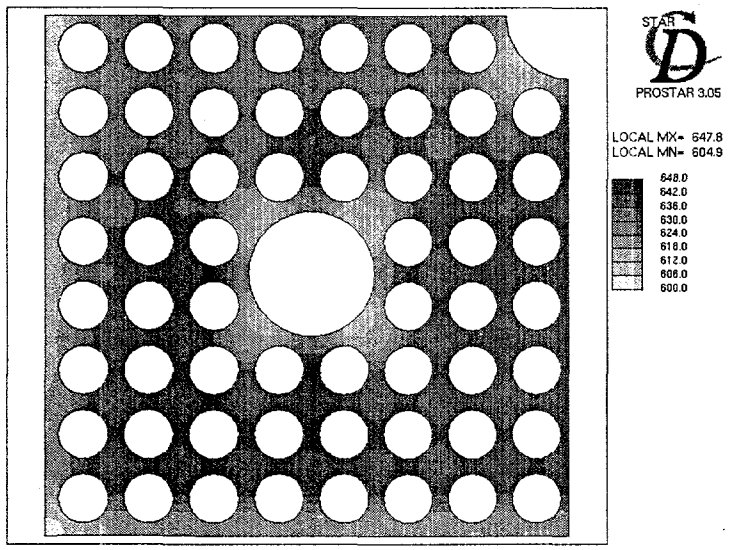

Figure 6. Temperature contours at outlet plane from STAR-CD for quarter subassembly

The change in the outlet temperatures predicted by STAR-CD high density model, when compared with the less-dense model, was minimal, indicating that the 473,600 cell model mesh density is adequate for the solution of this problem for the radial mesh density.

Our principal objective, however, is the demonstration of the capabilities of modern CFD codes in solving complex thermal-hydraulic problems. We have solved the flow and heat transfer in one-eighth of a reactor core using STAR-CD. The geometry, as viewed from above is shown in Figure 7. Each of the larger white circles seen in Figure 7 represents a control guide tube, while each of the smaller white circles represents a fuel rod.

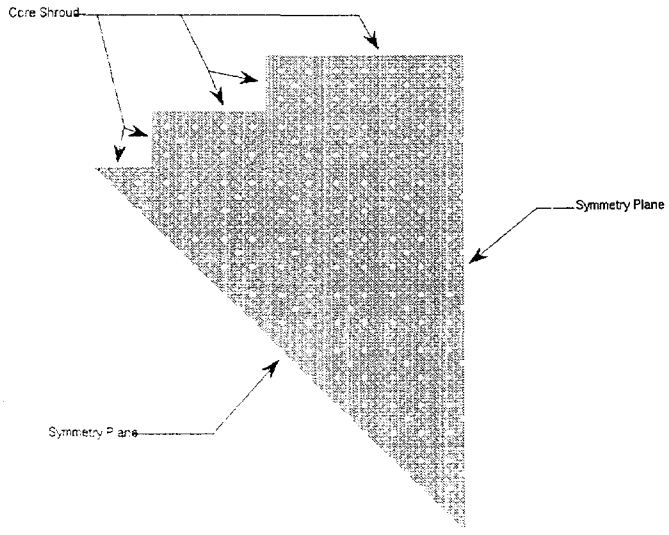

Figure 7. Geometry for 1/8 Reactor Core analysis using STAR-CD

In this study, we have extended our preliminary investigation to include modeling of important geometric characteristics of actual fuel assemblies. In particular, modern assembly designs include mixing vanes and spacer grids, as illustrated in figure 8 [Millstone Nuclear Power Station 1972]. In the particular core being studied in this investigation, there were 11 spacer grid/mixing vane structures. Since these structures are present to enhance thermal mixing among the intra-subassembly sub-channels, their effect is primarily in the axial direction, downstream of the spacer/vane. To help capture these effects, the axial meshing was refined by a factor of 4 from the original preliminary investigation.

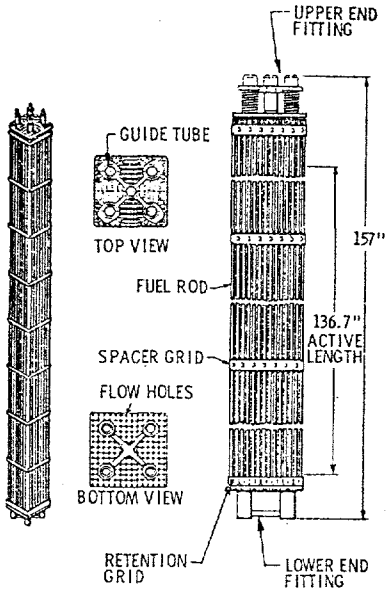

Figure 8. Fuel Assembly

As will be discussed in the next section, a mechanistic model of the effects of such structures can be determined from first principles. In this investigation, however, these structures were represented as porous media that relate pressure drop to flow rate as follows:

$$dP/dx_i = - (\alpha_i |U_i| + \beta_i) U_i \qquad (1)$$

where P is the pressure drop, x_i (i = 1,2,3) are the three principle directions of the global coordinate system, U_i are the velocity components in these three directions, and α_i and β_i are user-defined constants. As a convention, we will assume here that i = 3 represents the fuel pin axial direction and that i = 1,2 are any other two directions which are orthogonal to each other and the i = 3 direction.

To estimate values for the α_i and β_i to be used in this analysis, we first assumed that all $\alpha_i = 0$. This was done to promote stability of the solution, since $\alpha_i \neq 0$ in equation (1) represent non-linear terms. Second, β_3 was computed by assuming that the entire pressure drop across the core (which was known) occurred only across the eleven spacer grids (i.e. the pressure drop between spacer grids was assumed to be negligible). Then, knowing the spacer grid height and the average velocity, a value of β_3 was computed using equation (1). Finally, since the cross-stream (i = 1,2) velocities within the spacer grids are expected to be small, it was assumed that $\beta_1 = \beta_2 = 10\ \beta_3$.

The one-eighth core model has a mesh density similar to that shown in Figure 2, and consists of a total of 240,222,348 computational cells (837 layers in the axial direction by 287,004 cells per layer). Assembly power factors typically seen during a burnup cycle were used together with the pin radial power factors from the quarter subassembly analysis to specify a heat flux distribution on each of the more than 7,000 fuel pins represented in the model. The assembly power levels used in the analysis ranged from 21% to 138% of the average assembly power level.

In addition, the flow to each of the 30.125 assemblies was specified independently, ranging from 89% to 108% of the average assembly flow rate. In order to facilitate direct comparison with the quarter subassembly, the power and flow conditions in one assembly of the one-eighth core calculation at the hot assembly position, were the same as in the quarter subassembly calculation.

The analysis was performed in parallel on 200 IBM SP processors having a clock speed of 222 MHz. Twenty-five 8-way nodes (i.e. eight processors per node) were used. Each node had at least 4 GB of RAM. Communication between nodes is accomplished via a high-speed switch, resulting in an analysis that used a combination of shared and distributed memory.

The memory requirement for each single precision STAR-CD executable file was approximately 900 MB. File I/O was from/to a large shared file system having a capacity of approximately 250 GB.

A converged solution was obtained using approximately 58 hours of CPU time per process. Assembly of the STAR-CD output data files was performed layer-by-layer for the regions of interest, since assembly of the output data files for all 200 processors would have resulted in a file of unmanageable size (~ 40 GB).

The results of the analysis are displayed in figures 9 to 14. Figure 9 shows contours of temperature at the outlet plane near the assembly corresponding to that of the quarter subassembly calculation. In fact, the quarter subassembly in the center of Figure 9 may be compared directly to the quarter subassembly results of the previous section. It can be clearly seen that the temperatures in the neighboring assembly to the left are much lower, due to the much lower power and higher flow in that assembly.

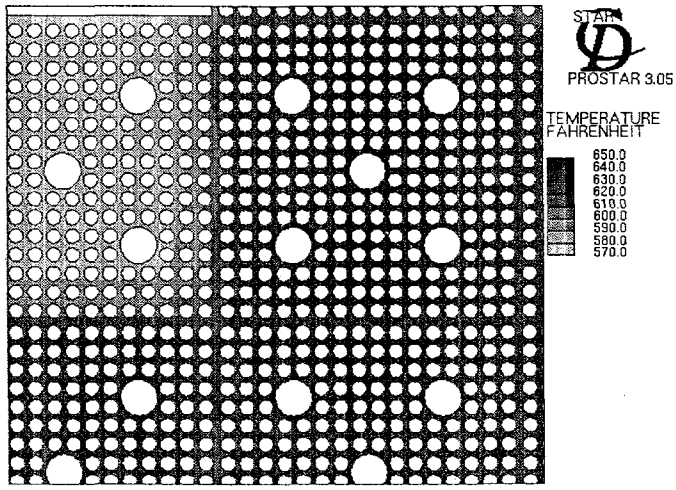

Figure 9. Temperature at the outlet plane near quarter subassembly from 1/8 core calculation

The effects of these differing flow and power levels may be seen in Figure 10, where the in-plane velocity components at the outlet plane are plotted. It is seen that there can be some inter-assembly flow, which can be attributed to both the differing flow rates of the various assemblies, and coolant thermal expansion effects. Note, however, that the magnitudes of these velocities are small compared to the velocities in the axial direction.

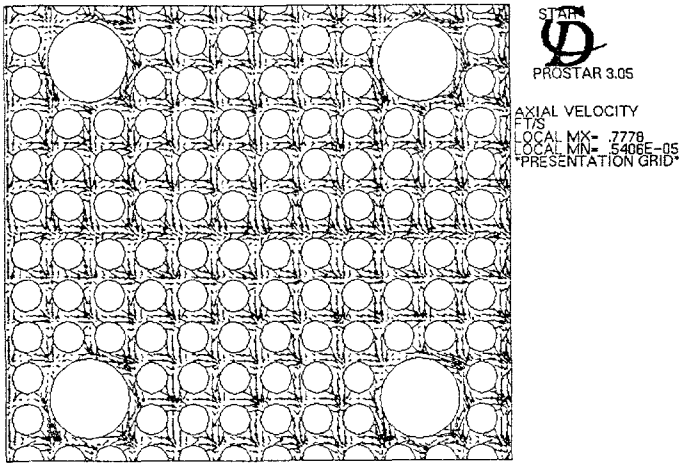

Figure 10. In-plane velocity at the outlet plane from 1/8 core calculation

Finally the resulting average subchannel temperatures are shown in Figure 11. In this figure the VIPRE results shown are those for the quarter subassembly described in the preceding section. The result of the inter-assembly flow sharing is seen to be generally lower peak temperatures. Although we have not used the pin by pin power for the whole core, we believe qualitatively the results have the right trend. Therefore, it may be concluded that it is important to accurately predict the temperatures in all assemblies simultaneously. CFD methodologies like those used by the STAR-CD code make such calculations practical.

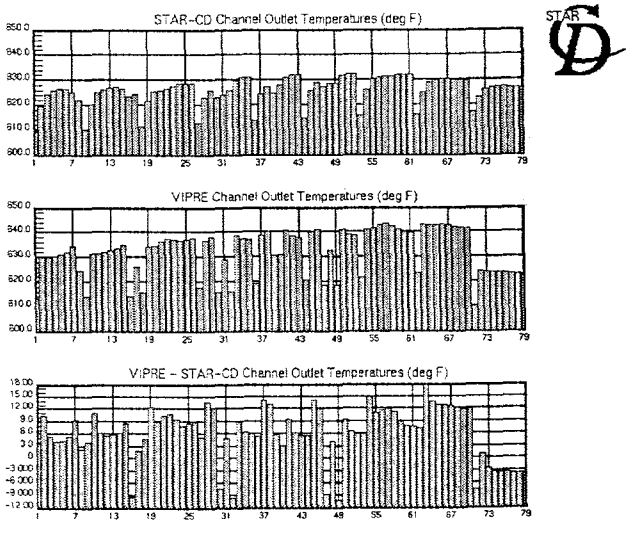

Figure 11. Average quarter sub-channel temperature comparison using STAR-CD 1/8 core analysis

The numerical studies performed were focused on establishing the conservatism that may be present when setting operating conditions due to the use of simplified models. This aspect can be illustrated by the data presented in Table 1. In the table, we have presented a summary of the peak outlet temperature in the hot quarter assembly. As can be seen, the use of higher fidelity models, even without proper account of the spacers, results in predictions of lower temperatures. With our porous media representation of the grids, even lower peak temperatures are predicted.

Table 1. Summary of Analyses and Peak Temperature in Hot Quarter Subassembly

Analysis	Model Size	No. Processors	Peak Temp. (F)
VIPRE			644
1/8 Core (w/o spacers)	57,400,800	64	639.8
1/8 Core (w/spacers)	68,019,948	64	633.4
1/8 Core (w/spacers)	240,222,348	200	634.4

It should also be observed that CFD calculations such as these provide much greater detail on the thermal hydraulic patterns. Codes like VIPRE cannot predict the spatial variation within channels. However, codes like STAR-CD can provide the detailed flow and temperature fields within the computational domain. As mentioned earlier, these detailed profiles can be used to investigate if temperature at the clad surface and in the water film adjacent to the clad surface are high enough to initiate bubble nucleation and hence precipitate crud buildup (which might be the cause of the axial offset anomaly).

Thermal design of reactor core fuel subassemblies is dictated by the need to prevent cladding failure and loss of fuel integrity during normal and off-normal operating conditions. This is in practice observed by the establishment of thermal margin to burnout conditions determined by the critical heat flux (q_{CHF}). For PWRs the margin to critical heat flux is maintained by specifications on the minimum allowable DNBR (departure from nucleate boiling ratio) where

$$DNBR = \frac{q_{CHF}}{q} \tag{2}$$

Significant effort over the last few decades have been devoted by the nuclear power industry, vendors, universities and government laboratories to the development of correlations, semi-empirical and empirical, for the prediction of q_{CHF} based upon geometrical factors, thermal-hydraulic conditions and fuel rod power shapes. Various correlations are currently in use. However, the main schemes are based either on the local condition hypothesis or on an integral approach. The local conditions hypothesis assumes that only the local conditions of heat flux and quality control DNB while the integral approach assumes that the upstream history is the determining factor. One local-condition-hypothesis based correlation, available in the open literature, is the one developed by Biasi et al [Biasi 1967]. The Biasi correlation consists of two equations, one for high quality and one for low quality. The equation that calculates the larger heat flux is selected for application. The equations are

$$q_{CHF-B=} \frac{1.883x10^7}{D_h^n G^{1/6}} \left[\frac{f(P)}{G^{1/6}} - X(Z) \right] \tag{3}$$

for the low-quality region, and

$$q_{CHF-B}\frac{3.78x10^{7}h(P)}{D_h^{n}G^{0.6}}[1-X(Z)] \tag{4}$$

for the high-quality region,

where

q	=	heat flux (W/m^2)
$X(Z)$	=	quality at location Z
D_h	=	hydraulic diameter (m)
G	=	mass velocity (kg/m^2s)

$$n=\begin{cases}0.4, for D_h \geq 1cm\\ 0.6, for D_h < 1cm\end{cases}$$

f(P)	=	$0.7249 + 0.099\ P\ e^{(-0.032P)}$
h(P)	=	$1.159 + 0.149\ P\ e^{(-0.019P)} + 8.99P/(10.+P^2)$
P	=	pressure (bar)

The equations were developed by fitting data for flow inside circular tubes over a range of parameters. While the correlation is not based on rod bundle data, it has been compared against rod bundle data and is reasonably good where the local equilibrium quality is well known. Since vendor proprietary CHF correlations utilized in specific licensing type design calculations were not generally available, in the open literature, the Biasi correlation was used in this particular study to illustrate the prediction of DNBR along the axial length of a fuel pin. The channel cross-section average quality is used in eqs. (3) and (4) as this is consistent with the experiments.

In Figure 12, we illustrate the use of this correlation, based on the calculated STAR results, which were obtained from the STAR-CD analysis using the correlations presented above. Data for pressure and heat flux along as a function of axial distance along the hot pin were output from the STAR-CD analysis as a post-processing operation. The pressure data were then used to compute the critical heat flux from the Biasi correlations above. Since the STAR-CD analysis did not include multiphase flow effects, it was assumed that the quality was zero everywhere along the hot pin. The critical heat flux was then used together with the STAR-CD heat flux data to compute the DNBR.

3.3 Reactor Core Fluid Dynamics

CFD analysis tools like STAR CD can obviously be of value in assessing thermal performance as illustrated in the section above. In addition, they provide a wealth of information that may be useful from other design perspectives. An example of this is the effect of cross flow. This is an important effect from a thermal perspective that can be captured from first principles if the flow

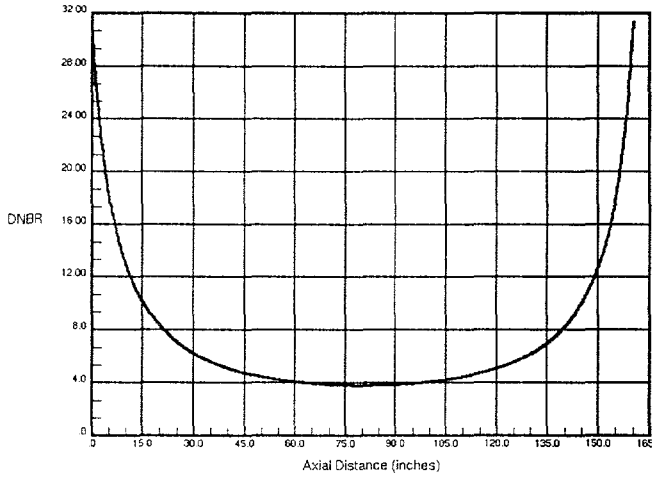

Figure 12. DNBR for Hot Sub-Channel of Hot Sub-Assembly

geometry is known. In addition, it is believed that important fuel rod vibration effects can be the result of this inter-subassembly flow. Since this geometry can be determined from a knowledge of the thermal and irradiation operating conditions, it is a straightforward application of CFD methodology to perform this analysis using actual 3-D geometry. Although the geometry may be bowed, the use of the unstructured mesh capability of STAR makes this modeling task straightforward. Although this was not done in this investigation, some of the effects of cross flow can be illustrated from part of the calculation.

In the analysis performed as part of this study, the inlet flow velocities were provided by the plant operator. These conditions typically vary from subassembly to subassembly to insure a flat power to flow ratio across the core. Due to this non-uniform inlet flow, which takes place physically due to a combination of inlet effects that are not in the current model, flow and pressure gradients exist, which will lead to inter-subassembly flows. Flow patterns at the inlet plane are indicated in Figures 13 and 14. It can be seen that a significant "radial" flow pattern exists at the inlet.

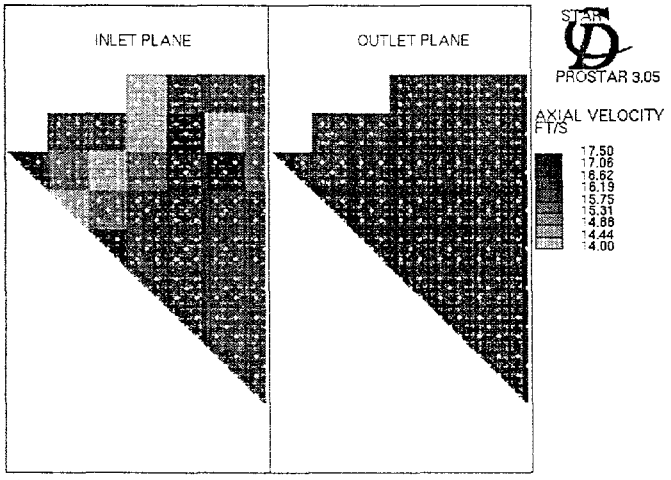

Figure 13. Axial Velocity Distributions at Inlet and Outlet Planes

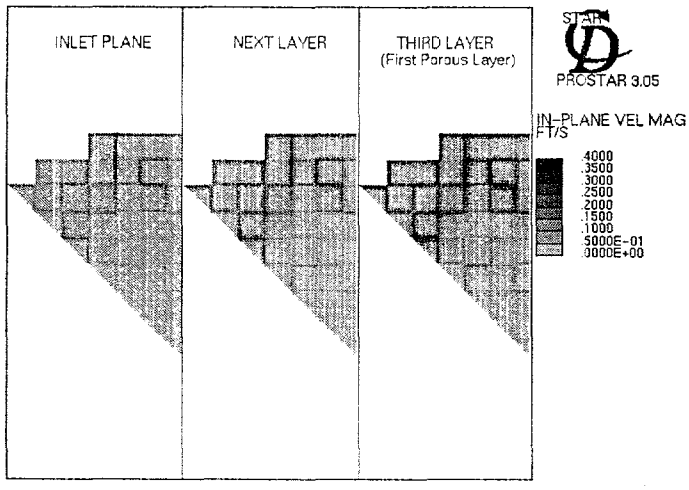

Figure 14. In-Plane Velocity Magnitudes Near Inlet

Although these effects are small for the configuration used in this analysis, substantial bowing effects are normally present under actual operating conditions in power reactors. These bowing effects are primarily due to thermal gradients, which are directly related to power distributions. These effects would typically take place in the hottest regions, reducing available flow to these assemblies, resulting in even greater bowing. At steady state conditions, the resulting bowing patterns can be significant, altering intra- as well as inter-subassembly flow patterns. Integrated thermo-mechanical analysis to predict these bowing patterns and their feedback effects are now possible with the use of CFD codes like STAR-CD coupled to structural analysis codes.

3.4 Spacer Grid/Mixing Vane Analysis

In the whole core subchannel analysis described in the previous section, an approximate representation of the spacer grids and mixing vanes was used. These structures play an important role in minimizing local hot spots within an assembly and between assemblies. As will be illustrated here, the details of these components can be analyzed with the assistance of high fidelity CFD. The scale of the mixing phenomena, however, is quite small and the use of high fidelity turbulence models and fine resolution computational grids is required. Proper representation of the grids requires several million nodes, making it practically impossible to include this level of modeling detail for whole core calculations. Nonetheless, these components are critical to operating reactors and the approach illustrated below will illustrate how CFD can be used to assess their performance.

The results of the detailed spacer grid analysis may be used to compute parameters used in a porous media representation of the spacer grids, for use in a larger (e.g. full core) model of the reactor. The procedure for computation of these parameters is as follows. The detailed spacer grid model was analyzed with a fixed mass flow rate. From this, the pressure drop across the spacer grid was computed by STAR-CD. The porous media representation of a fluid domain may be expressed mathematically using equation (1). Results of detailed spacer grid analyses at different flow rates can be used to fit a curve of the form of equation (1) to obtain α and β. These coefficients are then used in the porous media spacer grid representation of the full core reactor model.

To perform the detailed spacer grid/mixing vane analysis, the computational mesh was generated using samm (semi-automatic meshing methodology). It employs "trimmed cell technology" to produce a high quality mesh which consists predominately of hexahedral cells. Given a CAD surface definition of the domain to be analyzed, construction of the mesh using samm consists of the following steps: the generation of a subsurface a specified distance away from the surface, the generation and trimming of a hexahedral mesh to conform with the domain defined by the subsurface, and the extrusion of one or more cells layers from the mesh to the original surface definition.

A model and the computational grid of a typical 25 fuel pin model arranged in a 5x5 grid generated using this approach is illustrated in Figure 15a and 15b. For this model, the total number of computational cells was approximately 13 million. Since the goal of the analysis was to model the periodically fully developed flow through a spacer grid, one repeatable axial section around a single spacer grid was modeled. Logarithmic wall functions were used to specify the turbulence wall boundary conditions and the standard k-ε model was used to model turbulence in the main flow. Note that a single 'extrusion layer' was created adjacent to all solid surfaces to provide for accurate calculation of the near-wall turbulence conditions by the wall function models.

In order to resolve the details of the secondary flows generated by the mixing vanes, a second-order bounded scheme called MARS [STAR-CD V3.10 1999] was used for the spatial differencing of the convective terms.

Fixed heat flux wall thermal boundary conditions were applied to the pin surfaces. The flow boundary conditions were specified mass flow rate and average inlet temperature with cyclic boundaries. STAR-CD cyclic boundaries have the effect of coupling the inlet and outlet distributions of the field variables. In the case of the velocity components, the values are identical

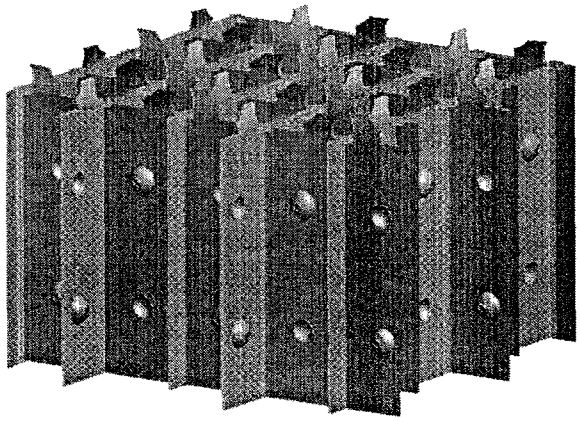

Figure 15a. Geometry of the Spacer Grid and Mixing Vanes

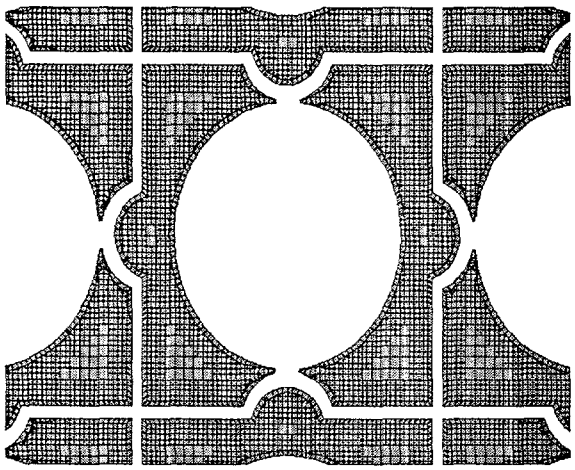

Figure 15b. Computational Mesh at a Section through Spacer Grid

at corresponding locations at the inlet and outlet planes, and the velocity components normal to these planes are scaled to maintain the specified mass flow rate. For the temperature, an average (or "bulk mean") temperature is specified at the inlet plane, with the inlet temperature distribution coupled to the outlet plane distribution. The outlet temperature level is determined by the solution of the energy conservation equation together with the specified wall thermal boundary conditions.

The analysis was performed in parallel on 16 IBM SP processors having a clock speed of 160 MHz. The memory requirement for each executable file was approximately 520 MB and a converged solution was obtained using about 60 CPU hours per process.

The results of the analysis are shown in Figures 16 and 17. Figure 16 shows the swirling flow developed as the coolant flows through the spacer grid, and especially, past the vanes. This swirling flow is seen to persist at least 0.2 meters downstream of the vanes, although its magnitude has decreased somewhat. The temperature contours in Figure 17 shows the effect of the mixing on the boundary layer adjacent to the fuel rods. In Figure 17a, which is a section plot just upstream of the spacer grid, well-defined thermal boundary layers are seen around each tube. As the coolant flows through the spacer grids and past the vanes, the swirling flow develops, destroying the boundary layers and lowering the temperature at the fuel rod surface, as shown in Figures 17b-d.

3.5 Scaling and Numerical Performance

Although parallel scaling studies were not done for any of the analyses presented in this paper, previous experience using STAR-CD on parallel platforms indicates the type of behavior that would be expected. Figure 18 shows the parallel scaling for passenger vehicle ventilation analyses using STAR-CD on two different computer platforms (labeled A and B). For relatively small numbers of processors (up to about eight), both machines show approximately linear speedup, although the two lines diverge somewhat due to the increasing communications overhead. For larger numbers of processors, Machine B follows the same trend while Machine A exhibits superlinear speedup. This superlinear speedup is due to the fact that Machine B uses the additional available memory as cache. This occurs when the available memory per processor is fixed while the analysis is performed on larger numbers of processors.

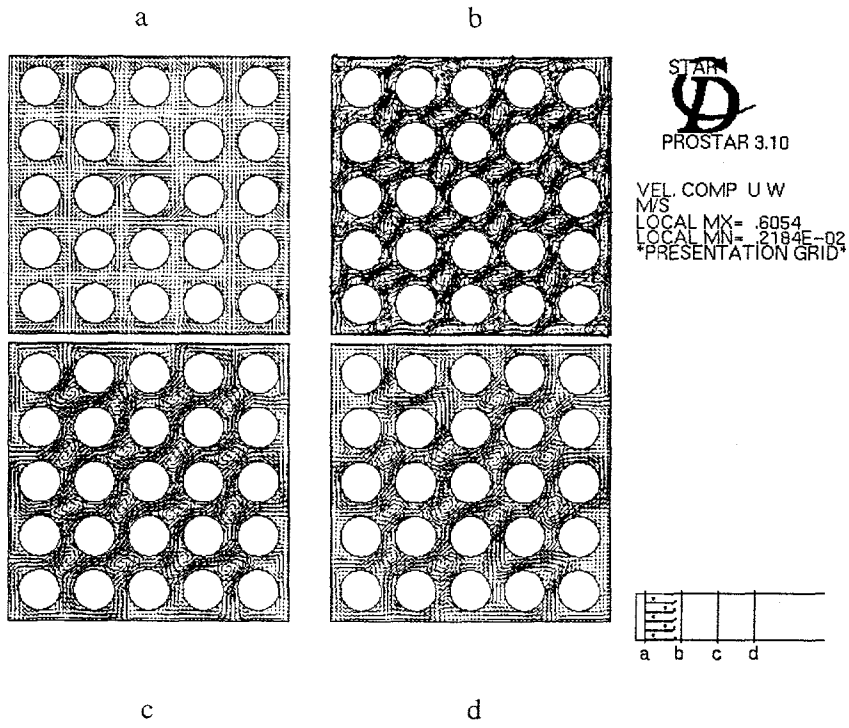

Figure 16. In-Plane Velocity Distribution at Various Axial Locations: (a) just upstream of the spacer grid; (b) just downstream of the mixing vanes; (c) 50 mm downstream of the mixing vanes; (d) 100 mm downstream of the mixing vanes

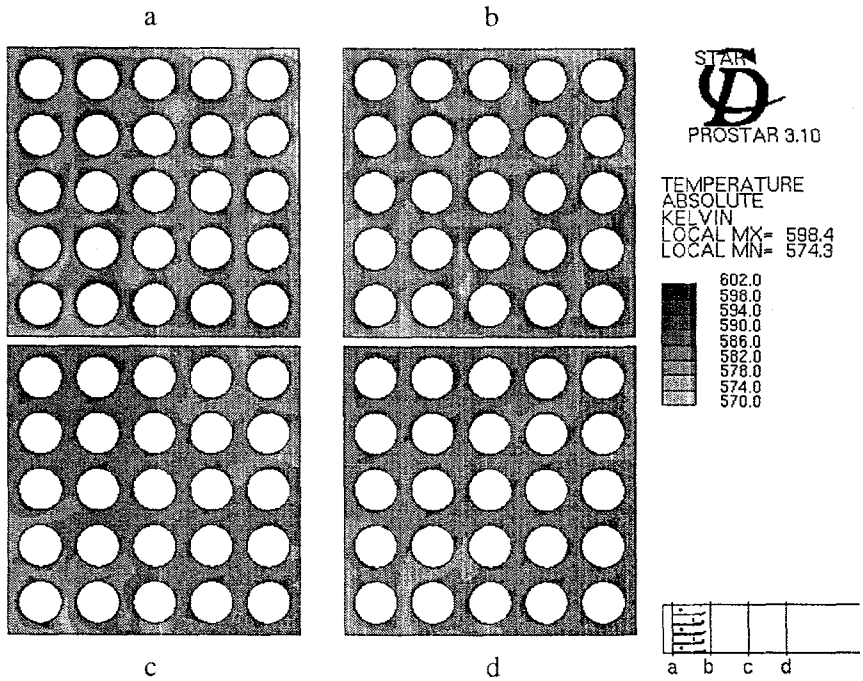

Figure 17. Temperature Distribution at Various Axial Locations:
(a) just upstream of the spacer grid; (b) just downstream of the mixing vanes;
(c) 50 mm downstream of the mixing vanes; (d) 100 mm downstream of the mixing vanes

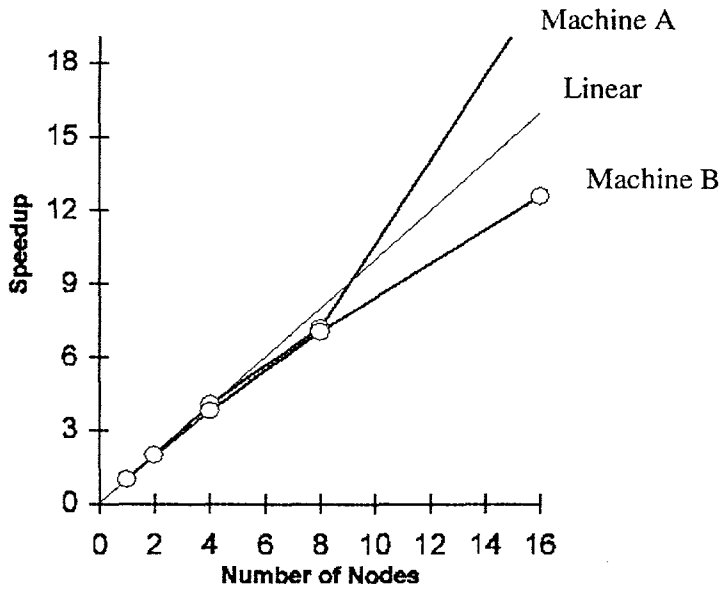

Figure 18. Parallel Performance of Passenger Vehicle Ventilation Analyses using STAR-CD

4 Conclusion

This paper has illustrated the use of modern computational fluid dynamics and high performance computers for nuclear reactor design. We have demonstrated the ability to perform high fidelity CFD analysis, which can provide the designer detailed information on operating characteristics and potential conservatism in operations. The power of massively parallel computing has also been illustrated with the 240 million node CFD calculation. These calculated results provide detailed information for assessing thermal and thermo-mechanical issues that were not possible with more simplified approached. It was also illustrated that the same high fidelity CFD approach can be used to assess the performance of key thermal-hydraulic components, such as spacer grids and mixing vanes. These CFD techniques can thus provide a self-consistent analysis methodology for understanding and designing key components and the systems they affect.

Acknowledgements

We would like to acknowledge the assistance of Mr. Larry Hwang of Nuclear Fuel Management at Palo Verde Nuclear Generating Station in formulating test problems for reactor subchannel analysis.

We would also like to acknowledge the IBM Corporation for allowing the use of their RS/6000 SP computer systems at the RS/6000 Benchmark and Enablement Center in Poughkeepsie, NY to analyze the 240 million cell reactor problem. Special thanks go to Samad Moini, Vance Sutton and Lerone Latouche, all of IBM, for facilitating and supporting the use of these systems.

This work was performed under the auspices of the U.S. Department of Energy, Office of Technology Support Programs, under Contract No. W-31-109-ENG-38.

References

L. J. Agee, "Overview of Electric Power Research Institute Nuclear Safety Analysis Activities," Nuclear Technology, 121, March, 1998.

L. Biasi, et al., "Studies on Burnout Part 3," Energia Nucleare, 14 (9), 530-536, 1967.

W. J. Boatwright, D. W. Hiltbrand, and W. G. Choe, "TU Electric's Experiences with the Development and NRC Approval of a Reload Safety Analysis Methodology," Nuclear Technology, 121, March, 1998.

H. Chelemer, P. T. Chu, and L. E. Hochreiter, "THINC-IV – An Improved Program for Thermal-Hydraulic Analysis of Rod Bundle Cores," BNWL-1962, Battelle-Pacific Northwest Laboratories, March, 1976.

EPRI-NP-2511-CCM, "Mathematical Modeling, Vol. 1: VIPRE-01, A Thermal-Hydraulic Analysis Code for Reactor Cores," Electric Power Research Institute, Palo Alto, California, Prepared by Battelle, Pacific Northwest Laboratories, Richland, Washington, November, 1983.

J. H. Ferziger and M. Peric, "Computational Methods for Fluid Dynamics," Springer-Verlag, 1997.

Computational Dynamics, STAR-CD V3.10 Methodology Manual, London, UK, 1999.

O. J. Lang, J. Silvestri and B. Crawford, "Analysis of a Close-Coupled Catalyst by a Combined 1D/3D Calculation Model", Sixth Symposium of the Institute for Internal Combustion Engines and Thermodynamics, Graz University of Technology, September, 1997.

S. V. Patankar, "Numerical Heat Transfer and Fluid Flow," Hemisphere Publishing, 1980.

Millstone Nuclear Power Station, Final Safety Analysis Report, Vol. I, August, 1972.

G. B. Swindlehurst, "A Utility Perspective on Subchannel Analysis," Nuclear Technology, 112, December, 1995.

"TORC-Code: A Computer Code for Determining the Thermal Margin of a Reactor Core, CENPD-161, ABB CE Topical Report, July, 1975.

D. P. Weber, et al, "Computational Fluid Dynamics (CFD) and Its Potential for Nuclear Applications," presented at: The American Power Conference, Chicago, IL, April, 1999.

C. L. Wheeler, et al., "COBRA-IV: An Interim Version of COBRA for Thermal Hydraulic Analysis of Rod Bundle Nuclear Fuel Elements and Cores," BNWL-1962, Battelle-Pacific Northwest Laboratories, March, 1976.